# Air-sea CO$_2$ fluxes and the controls on ocean surface $p$CO$_2$ seasonal variability in the coastal and open-ocean southwestern Atlantic Ocean: A modeling study

Ricardo Arruda[1], Paulo H. R. Calil[1], Alejandro A. Bianchi[2,3], Scott C. Doney[4], Nicolas Gruber[5], Ivan Lima[4], and Giuliana Turi[5,6]

[1]Laboratório de Dinâmica e Modelagem Oceânica (DinaMO), Instituto de Oceanografia, Universidade Federal do Rio Grande, Rio Grande, RS, Brazil.
[2]Departamento de Ciencias de la Atmósfera y los Oceános, Universidad de Buenos Aires, Buenos Aires, Argentina.
[3]Departamento Oceanografía, Servicio de Hidrografía Naval, Av. Montes de OCA2124- Buenos Aires, Argentina
[4]Department of Marine Chemistry and Geochemistry, Woods Hole Oceanographic Institution, Woods Hole, MA, USA.
[5]Institute of Biogeochemistry and Pollutant Dynamics, ETH Zurich, Zurich, Switzerland.
[6]Now at: CIRES, University of Colorado at Boulder, and NOAA/ESRL, Boulder, CO, USA.

*Correspondence to:* Ricardo Arruda (cadoarruda@gmail.com)

**Abstract.** We use an eddy-resolving, regional ocean biogeochemical model to investigate the main variables and processes responsible for the climatological spatio-temporal variability of $p$CO$_2$ and the air-sea CO$_2$ fluxes in the southwestern Atlantic Ocean. Overall, the region acts as a sink of atmospheric CO$_2$ south of 30°S, and is close to equilibrium with the atmospheric CO$_2$ to the north. On the shelves, the ocean acts as a weak source of CO$_2$, except for the mid/outer shelves of Patagonia, which act as sinks. In contrast, the inner shelves and the low latitude open ocean of the southwestern Atlantic represent source regions. Observed nearshore-to-offshore and meridional $p$CO$_2$ gradients are well represented by our simulation. A sensitivity analysis shows the importance of the counteracting effects of temperature and dissolved inorganic carbon ($DIC$) in controlling the seasonal variability of $p$CO$_2$. Biological production and solubility are the main processes regulating $p$CO$_2$, with biological production being particularly important on the shelves. The role of mixing/stratification in modulating $DIC$, and therefore surface $p$CO$_2$, is shown in a vertical profile at the location of the Ocean Observatories Initiative (OOI) site in the Argentine Basin (42°S, 42°W).

## 1 Introduction

Shelf regions are amongst the most biogeochemically dynamical zones of the marine biosphere (Walsh, 1991; Bauer et al., 2013). Even though they comprise only $7 - 10\%$ of the global ocean area (Laruelle et al., 2013), continental shelves could contribute to approximately $10 - 15\%$ of the ocean

primary production and $40\%$ of the ocean's carbon sequestration through particulate organic carbon (Muller-Karger et al., 2005). Global discussions about the role of continental margins as a sink of atmospheric $CO_2$ gained momentum after Tsunogai et al. (1999) suggested that these shelf regions take up as much as 1 PgC/year of atmospheric $CO_2$. Recent estimates range from 0.2 PgC/year (Laruelle et al., 2013) to roughly 0.6 PgC/year (Yool and Fasham, 2001), somewhat more modest than initially thought (Gruber, 2015), but still relevant to the global ocean sink estimated around 2.3 PgC/year (Ciais et al., 2014).

Continental shelves tend to act as a sink of carbon at high and medium latitudes ($30° - 90°$), and as a weak source at low latitudes ($0° - 30°$) (Chen et al., 2013; Hofmann et al., 2011; Bauer et al., 2013; Laruelle et al., 2014), i.e., they tend to follow similar meridional trends as the open ocean $CO_2$ fluxes (Landschützer et al., 2014; Takahashi et al., 2009).

However, continental shelves present a higher spatio-temporal variability of air-sea $CO_2$ fluxes than the adjacent open ocean, with the inner shelf and near coastal regions generally acting as a source of $CO_2$ to the atmosphere, while the mid/outer shelf and the continental slope generally act as sinks (Cai, 2003). This pattern can be explained by the increased primary production and decreased terrestrial supply towards the outer shelf (Walsh, 1991). Seasonality of the upper ocean (e.g. mixing and stratification) may also be important to the air-sea exchange of carbon. For example, the United States southeast continental shelf acts as a sink of $CO_2$ in the winter and as a source in the summer (Wang et al., 2005).

In the southwestern Atlantic Ocean, the shelf region presents distinct features. To the south, the Patagonian shelf is one of the world's largest shelves with an area close to $10^6$ km$^2$, broadening to more than 800 km from the coastline (Bianchi et al., 2009). To the north, the Brazilian shelf narrows to around 100-200 km from the coastline. This region is one of the most energetic regions of the world's ocean with the confluence of the warm southward-flowing Brazil Current (BC) and the cold Malvinas Current (MC) flowing northward (Piola and Matano, 2001). The extension of the confluence roughly divides the subtropical and subantarctic oceanic gyres in the South Atlantic and might be a hotspot for shelf-open ocean exchange (Guerrero et al., 2014).

In the open-ocean, the South Atlantic is thought to absorb between 0.3-0.6 PgC/year south of $30°$S, while acting as a source to the atmosphere north of $30°$S (Takahashi et al., 2002). Aside from global open-ocean estimates, only a few local studies were conducted on the continental shelves in this region. The Patagonia shelf was characterized as a source of $CO_2$ to the atmosphere on the inner shelf, and as a sink in the mid-outer shelf (Bianchi et al., 2009). The southeast Brazilian shelf and continental slope were characterized as sources of $CO_2$ to the atmosphere during all seasons (Ito

2

et al., 2005). Such regions are often neglected, or poorly resolved, on relatively coarse global modelling assessments, although they may contribute up to 0.2 PgC/year of global ocean $CO_2$ uptake (Laruelle et al., 2014).

Regional marine biogeochemical models have been used to assess the ocean carbonate system and $CO_2$ fluxes, including the continental margins. For example, along the US east coast, the seasonality of $p CO_2$ was found to be controlled mainly by changes in the solubility of $CO_2$ and biological processes (Fennel and Wilkin, 2009). Along the California coast, biological production, solubility and physical transport (e.g. circulation) were found to be the most influential processes on $p CO_2$ variability, both spatially and temporally (Turi et al., 2014).

In this study we use a regional marine biogeochemical model coupled to a hydrodynamic model to investigate the parameters and processes regulating the variability of ocean surface $p CO_2$ in the southwestern Atlantic Ocean. Our model domain includes the location of the global node mooring that is soon to be deployed as part of the Ocean Observatories Initiative (OOI) at 42°S, 42°W (oceanobservatories.org).

We compare modeled surface $p CO_2$ distribution with observations and use the results to investigate the relative importance of the parameters ($DIC$, temperature, alkalinity and salinity) and processes (biological production, air-sea $CO_2$ flux, $CO_2$ solubility and physical transport) in controlling surface $p CO_2$ distribution and variability on the continental shelf and open ocean in the southwestern Atlantic Ocean.

## 2   Materials and Methods

### 2.1   Model

The physical model used in this study is the Regional Ocean Modeling System (ROMS) (Shchepetkin and McWilliams, 2005). Our model domain spans from 15°S to 55°S, and from 70°W to 35°W, i.e., covering the southwestern Atlantic from its subtropical to subantarctic latitudes and from the continental shelf all the way out to the open ocean. The horizontal grid resolution is 9 km, with 30 vertical levels with increasing resolution towards the surface.

The biogeochemical model is an NPZD type, including the following state variables: phytoplankton, zooplankton, nitrate, ammonium, small and large detritus, and a dynamic chlorophyll to carbon ratio for the phytoplankton (Gruber et al., 2006). A carbon component is also coupled to the model, with the addition of calcium carbonate, $DIC$ and alkalinity to the system of state variables (Gruber

90 et al., 2011; Hauri et al., 2013; Turi et al., 2014). Parameters ~~utilised~~ in the biogeochemical model are listed in Table 1 of Gruber et al. (2006), ~~and the~~ $CaCO_3$ ~~parameters~~ as in Hauri et al. (2013). ~~These parameters represent~~ phytoplankton types ~~with~~ large nutrient requirements and relatively fast growth rates, ~~usually large organisms~~ (Gruber et al., 2006). Since our domain encompasses several ecological provinces (Gonzalez-Silvera et al., 2004), we may not represent all regions equally well

95 with only one phytoplankton functional type.

The initial and boundary conditions used for the physical variables were obtained from a climatology of the Simple Ocean Data Assimilation (SODA) (Carton and Giese, 2008), and for the biogechemical variables from a Community Earth System Model (CESM) climatological model

100 product (Moore et al., 2013). The model is forced at the surface with climatological winds from QuikSCAT (Risien and Chelton, 2008) and heat and freshwater surface fluxes from the Comprehensive Ocean-Atmosphere Data Set (COADS) (Da Silva et al., 1994). We used a fixed atmospheric $pCO_2$ of 370 $\mu$atm without $CO_2$ incrementation throughout the years and without seasonal variations. ~~Starting from rest we~~ ran the model for 8 years and used a climatology from years 5 through 8

105 ~~for~~ our analyses.

Even though ~~some~~ processes as river runoff and tides are locally relevant (i.e., la Plata River, and Patagonia shelf), we are not considering them in the present study (see conclusions section). The low salinity waters from the La Plata river are included in the climatological forcing from COADS

110 which are "nudged" into the model. These shortcomings may effect the results in some regions, but it is unlikely that they will affect the overall $pCO_2$ results in the wider domain.

## 2.2 Analysis

Ocean surface $pCO_2$ is the most important variable determining the air-sea $CO_2$ flux. This is because

115 the variability of ocean $pCO_2$ is much greater than that of atmospheric $pCO_2$, and variations in the gas transfer coefficient are usually several times smaller than those of ocean surface $pCO_2$ (Takahashi et al., 2002). Seawater $pCO_2$ is regulated by the concentration of dissolved inorganic carbon ($DIC$), alkalinity ($ALK$), temperature ($T$) and salinity ($S$). While $T$ and $S$ are controlled solely by physical factors, $DIC$ and $ALK$ are affected both by biological production and physical transport.

120 $DIC$ concentration is also affected by air-sea $CO_2$ fluxes (Sarmiento and Gruber, 2006).

In our model, ocean surface $pCO_2$ is calculated through a full model implementation of the seawater inorganic carbon system, i.e., as a function of the state variables $T$, $S$, $DIC$, and $ALK$, with the dissociation constants $k_1$ and $k_2$ from Millero (1995). In order to assess the impact of different

125 parameters on $pCO_2$ variability, we decompose $pCO_2$ with respect to $T$, $S$, $DIC$ and $ALK$, follow-

ing the approach of Lovenduski et al. (2007); Doney et al. (2009); Turi et al. (2014) and Signorini et al. (2013),

$$\Delta pCO_2 = \frac{\partial pCO_2}{\partial DIC}\Delta DIC^s + \frac{\partial pCO_2}{\partial ALK}\Delta ALK^s + \frac{\partial pCO_2}{\partial T}\Delta T + \frac{\partial pCO_2}{\partial FW}\Delta FW \qquad (1)$$

130 ,

where the $\Delta$'s are anomalies, either spatial or temporal, relative to a domain or an annual mean, respectively. $DIC^s$ and $ALK^s$ are the variable concentrations normalized to a domain-averaged surface salinity of 34.66, therefore effects from dilution of $DIC$ and $ALK$ through freshwater input

135 are not included in $DIC^s$ and $ALK^s$ terms. The dilution effect is considered instead in the freshwater component (FW) as it includes the effects of precipitation and evaporation on $DIC$ and $ALK$ concentrations.

The partial derivatives were calculated following Doney et al. (2009). $pCO_2$ was recalculated four

140 times adding a small perturbation to the spatial, or temporal, domain average for each variable ($T$, $S$, $DIC$, $ALK$) while maintaining the other 3 variables fixed to the domain averaged surface values. The perturbation applied here was 0.1% of the domain mean.

In order to investigate the parameters and processes controlling $pCO_2$ on the continental margin,

145 we limited our temporal analysis to three regions with depths shallower than 1000 m: the Southeast Brazilian Shelf (SEBS) in the northern part of the domain, the South Brazilian Shelf (SBS) in the middle of the domain that encompasses the Uruguayan Shelf, and the Patagonia Shelf (PS) to the south of the domain (Fig.1a). We also selected two open ocean regions for comparison with the continental shelves: a subtropical (ST) and a subantarctic (SA) region (Fig.1b). In each of these regions,

150 we estimated the monthly contribution of each parameter to the modeled $pCO_2$ variability by spatially averaging the parameters within each region, and using the temporal anomalies (subtracting the annual mean) on Eq. 1. For the spatial analysis, we used the whole study area and then calculated in each grid cell the spatial anomalies (subtracting the domain mean of that grid cell), finally applying it to Eq. 1.

155

In order to identify the main processes responsible for the variability of surface $pCO_2$, we used a progressive series of sensitivity experiments as in Turi et al. (2014), focusing on the processes of biological production, $CO_2$ solubility, air-sea $CO_2$ fluxes, and physical transport. To quantify these processes, we made three additional model runs, progressively excluding each process. In the first

160 experiment (E1), we set the $CO_2$ gas exchange flux coefficient between the atmosphere and the ocean to zero, inhibiting gas exchange in the surface layer. In the second experiment (E2), we started from

5

E1 and also turned off the photosynthetically available radiation (PAR), preventing phytoplankton growth. Finally, in experiment E3, the $CO_2$ solubility was set to a constant value, calculated with the domain-averaged surface salinity and temperature of 34.66 and 12.33 °C, respectively, while maintaining the changes of E1 and E2. The control run minus E1 represents the impact of gas exchange between ocean and atmosphere, E1 minus E2 represents the impact of biology, E2 minus E3 represents the impact of variable solubility. The last experiment (E3), in which there is no air-sea flux, no biology and constant solubility represents the impact of physical transport (Turi et al., 2014).

Given the short model integration times, the vertical gradients in the E3 simulation have not come in to steady-state with the processes. So our physical transport is working on the vertical $DIC$ gradients established by the biological pump. Since the lateral boundary conditions are the same for all experiments, these simulations are therefore only approximations of the impact of each process on $pCO_2$. Further, this separation assumes a linear additionality of each process, which is clearly a strong simplification given the non-linear nature of the inorganic carbonate system (Sarmiento and Gruber, 2006). The same spatial and temporal analysis described for the variables ($ALK$, $DIC$, $T$ and FW) was also applied for the processes experiments (air-sea $CO_2$ flux, biology, $CO_2$ solubility, physical transport).

## 3   Model Evaluation and Validation

Model results were evaluated against data from the Surface Ocean $CO_2$ Atlas (SOCAT) version 2 (Bakker et al., 2013). SOCAT $fCO_2$ observations were converted into $pCO_2$ using the set of equations from Körtzinger (1999) and then compared with modeled $pCO_2$ to assess the overall skill of the model. Due to the paucity of in-situ observations, particularly on the continental shelves, we used monthly climatologies for the comparison. The seasonal model evaluation was made over the whole domain (Fig.1). On the Patagonia Shelf, data from the Argentinian cruises ARGAU and GEF3 were used for a more focused comparison of the model results (Bianchi et al., 2009). For the Brazilian continental shelves no data were found for local comparisons.

Overall, our model simulates reasonably well the seasonality of ocean surface $pCO_2$, with the latitudinal and cross-shelf gradients represented during all seasons (Fig.2). Since our simulation has a fixed atmospheric $pCO_2$ of 370 $\mu$atm, this value separates the source from the sink regions. In the northernmost oceanic region, between 16°S and 30°S, the observations show $pCO_2$ close to $370 - 380$ $\mu$atm. Therefore this region acts as a weak source of $CO_2$ to the atmosphere. This tendency is well captured by the model, particularly during summer and autumn. From 30°S to 55°S, the whole offshore region acts as a $CO_2$ sink, with $pCO_2$ ranging from 250 $\mu$atm to 350 $\mu$atm during

6

all seasons in the model results. The observations show the same pattern down to $50°$S. However in the southernmost region the observed $pCO_2$ rises to values close to $400$ $\mu$atm. On the Southeast Brazilian Shelf, there were no data for model evaluation, but the overall behaviour of $pCO_2$ agrees with previous results from Ito et al. (2005), who suggested that the continental shelf in this region acts as a source to the atmosphere across both inner and outer shelves during all seasons. The southernmost and northernmost regions are where our model has the largest biases, underestimating the ocean surface $pCO_2$. These biases could be due to a variety of reasons, including the high variability of the Antarctic Circumpolar Current and/or proximity to the model boundary with potential biases in the lateral boundary conditions used to force the model.

On the Patagonia Shelf the model was evaluated using in-situ observations from Bianchi et al. (2009) during the years 2000 to 2006 (Fig.3). The model agrees very well with the seasonality of the observations of this shelf region, in particular the high $pCO_2$ values along the inner shelf, which make these regions a source of $CO_2$ during all seasons, but more intense during autumn/winter (Fig.3 b,c,f,g). In the mid-outer shelf the ocean generally acts as a sink, while to the north the ocean is in equilibrium with the atmosphere particularly during winter.

The monthly analysis was restricted to three offshore areas (A1, A2 and A3 in Fig.4a). We compared the spatial monthly mean modeled surface $pCO_2$ with the monthly average of the SOCAT $pCO_2$ data available in each area. Within these areas, we applied the following statistical indicators used in Dabrowski et al. (2014) in order to quantitatively assess model skill: model efficiency $ME = 1 - (\Sigma(O-M)^2)/(\Sigma(O-\bar{O})^2)$ (Nash and Sutcliffe, 1970), cost function $CF = (\Sigma \mid M-O \mid)/(n\sigma_o)$ (Ospar et al., 1998) and percentage of bias $PB = \mid (\Sigma(O-M).100)/\Sigma O \mid$ (Allen et al., 2007), where $M$ stands for modeled $pCO_2$ and $O$ for observations from SOCAT database, $n$ is the number of observations and $\sigma_o$ is the standard deviation of all observations. These statistics are indicators of the model's performance and provide complementary information of the model skill. ME relates model error with observational variability, CF is the ratio of mean absolute error to standard deviation of observations, and PB is the bias normalized by the observations (Dabrowski et al., 2014; Stow et al., 2009). Basically if $ME > 0.5$, $CF < 1$ and $PB < 20$, indicate that the model is "good/reasonable" when comparing to observations. If $ME < 0.2$, $CF > 3$ and $PB > 40$ the model is classified as "poor/bad ".

Modeled $pCO_2$ results for A1 agree very well with the observations, representing the $pCO_2$ evolution throughout the year with maximum values in summer (Fig.4b). All statistical indicators characterized the model with a good/reasonable skill in A1 (Table 1).

A2 is the region with the largest $pCO_2$ standard deviation from both model and observations (Fig.4c). This region is near the confluence between the warm Brazil Current and the cold Malvinas Current, generating one of the most energetic regions of the world's oceans. Moreover, this region comprises the shelfbreak front, with differences in stratification, local dynamics and salinity between shelf waters and Malvinas current waters (Fig.2a). Consequently, ME was estimated as poor/bad in this region, probably due to the high $pCO_2$ data variability. But CF and PB were both rated as "good/reasonable"(Table 1).

In A3 the model consistently underestimated $pCO_2$ (Fig.4d). This bias is seen in the seasonal comparison and in the monthly analysis, where summer is the only season for which modeled $pCO_2$ is within the standard deviation of the observations. ME was estimated as poor/bad in A3, but PB and CF rated our model as reasonable and good, respectively. (Table 1). Both A2 and A3 regions are close to an area of elevated eddy kinetic energy (Fig.4a), which could explain the large standard deviation and biases in these regions.

The Taylor diagram is consistent with the model efficiency (ME) estimate, showing good/reasonable results in A1, with a correlation of 0.8, and poor results in A2 and A3, with negative correlations (Fig.5). Only in A1, the correlation was found to be statistically significant. Aside from greater $pCO_2$ variability in these regions, the poor results found in A2 and A3 could also be due to the paucity of the observational data both in space and time.

Furthermore, in order to validate the baseline of our model, seasonal climatologies of modeled sea surface temperature and chlorophyll-a were compared with climatologies from AVHRR and MODIS-aqua, respectively. Results and a detailed discussion of this validation are shown in the appendix.

In conclusion, our model reproduces the most important north-south and inner-outer shelf gradients seen in the $pCO_2$ observations. While there is clearly room for improvement, we deem this level of agreement as sufficient for proceeding to the analysis of the processes and parameters affecting $pCO_2$ variability in this region.

## 4   Results and Discussion

### 4.1   $pCO_2$ drivers - spatial analysis

Modeled $pCO_2$ spatial anomalies relative to the domain average are shown in Fig.5a, with positive anomalies prevailing on the Brazilian continental shelves, inner-mid Patagonia Shelf and North

of 32°S, while the negative anomalies are found in the open ocean south of 32°S and in the mid-

270    outer Patagonia Shelf. $DIC^s$ has the highest impact on the spatial variations, being counteracted by $ALK^s$ and $T$ (Fig.6). In contrast, the fresh water flux has a minor influence on the spatial anomalies of $pCO_2$, agreeing with Turi et al. (2014) and Doney et al. (2009). ~~Even though with a~~ smaller role, ~~$ALK^s$~~ influence on $pCO_2$ anomalies ~~presented absolute values~~ higher (−100 to 100 μatm) than previous studies in other regions (Lovenduski et al., 2007; Turi et al., 2014). The higher contribution of both $DIC^s$ and $ALK^s$ to the spatial variations in $pCO_2$ could be explained by the more hetero-

275    geneous domain that encompasses several distinct surface water masses and frontal zones. Also, the elevated contribution of $ALK^s$ could be due to our relatively high $CaCO_3$ to biological production ratio of 0.07.

The changes in the state variables affecting $pCO_2$ are ultimately being driven by physical and bio-

280    geochemical processes. We investigate the role of each of these processes in controlling the changes in surface $pCO_2$ from our sensitivity experiments (E1, E2, E3). The most important processes affecting the spatial distribution of $pCO_2$ are biological production (E1 - E2) and physical transport (E3) (Fig.7). When physical transport (vertical and horizontal) is the only process altering $pCO_2$, we observe an increase in $pCO_2$ of up to 800 μatm on the continental shelves, due to the upwelling and

285    vertical mixing of $DIC$-rich subsurface waters. At the same time, the effect of biological production on the uptake of $DIC$ and changes in $ALK$ due to nitrate uptake and production/dissolution of $CaCO_3$ accounts for a decrease of up to −600 μatm on the continental shelves. Solubility effects (E2 - E3) are responsible for a decrease in $pCO_2$ south of 45°S and an increase in $pCO_2$ to the north, ranging from −50 to 50 μatm. Finally, air-sea $CO_2$ fluxes (Control - E1) have little impact on

290    regulating the ocean surface $pCO_2$. The effect of both biological production and physical transport is ~~maximal~~ on the continental shelves~~, with the~~ balance between these processes largely controlling ~~$pCO_2$ there. In~~ the open ocean, ~~physical transport largely controls $pCO_2$, again being counteracted by biological production~~. North of 45°S, biological production is ~~being~~ counteracted by physical transport and solubility, whereas ~~to the~~ south of 45°S physical transport is ~~being~~ counteracted by

295    biological production and solubility.

The strong effect of biological production on the shelf region is a result of the elevated nutrient supply and high primary production found in these regions, with increasing contribution towards the inner shelves. Physical transport presents a higher contribution on the continental shelves, where

300    the mixed layer often spans the entire water column, showing the importance of vertical mixing in bringing ~~metabolic~~ $DIC$ as well as nutrients to the surface waters, therefore increasing $pCO_2$. These results are in agreement with previous studies (c.f. Turi et al. (2014)), showing the importance of the biological net community production and advection of $ALK$ and $DIC$ (physical transport) in controlling ocean surface $pCO_2$. This suggests a major role of net community production in reducing

305  ocean $pCO_2$ in the region.

### 4.2  $pCO_2$ drivers - temporal analysis

In order to identify the seasonal variability of the contribution of each parameter, we used local grid temporal anomalies over the seasonal cycle (Fig.8). $DIC^s$ and $T$ are still the most influential param-

310  eters, with increasing importance on the continental shelves. The contribution by $ALK^s$ is relevant only on continental shelves south of $32°$S, and FW have a minor influence (not shown). It is important to highlight that the magnitude of the signals seen in this analysis is one order of magnitude smaller than the previous spatial analysis. This is likely due to our large and heterogeneous domain, which results in much spatial gradients than what is modeled over the seasonal cycle.

315

The contribution of the state variables in each continental shelf region (Fig.9) shows that these three regions have distinct characteristics, with different contributions from each parameter. In all three regions, $DIC^s$ and $T$ are the most important parameters affecting $pCO_2$ anomalies, albeit with opposing and seasonally varying contributions. While in summer the $T$ contribution increases $pCO_2$,

320  that of $DIC^s$ acts to diminish $pCO_2$. The opposite occurs in winter. The Southeast Brazilan Shelf (SEBS) is the region with the least variability in $pCO_2$ anomalies, with the contributions of both $DIC^s$ and $T$ in this region ranging from $-10$ $\mu$atm to $10$ $\mu$atm.

The South Brazilian Shelf (SBS) is the region with the largest variability in $pCO_2$ anomalies, with

325  $ALK^s$ having the most prominent impact on $pCO_2$ compared to the other regions - up to $15$ $\mu$ atm in spring. $DIC^s$ is the most important parameter in this area, with a contribution of up to $70$ $\mu$ atm, followed by temperature, with a contribution of up to $60$ $\mu$atm in the winter. On the Patagonia Shelf (PS) and South Brazilian Shelf (SBS), although the amplitude of the contributions by $DIC^s$ and $T$ are large, the tendency of these two terms to cancel each other out results in smaller $pCO_2$ anomalies.

330  In both SBS and PS, $pCO_2$ is predominately controlled by $T$ and $DIC^s$, with small contributions from ALK and FW.

Seasonal warming/cooling is largely controlling $pCO_2$ anomalies signals throughout the continental shelves, only being dampened by $DIC^s$, and also by $ALK^s$ in the case of the South Brazilian

335  Shelf (SBS). This pattern of seasonal variation of the parameters on continental shelves agrees with the results from Signorini et al. (2013) and Turi et al. (2014), although with different absolute values. The pattern of diminishing variability towards subtropical continental shelves is also shown by Signorini et al. (2013).

10

340     This pattern of opposing contributions of $T$ and $DIC$ was also found along the North American east coast by Signorini et al. (2013), who attributed winter mixing and the spring-summer biological drawdown as the processes responsible for $p\mathrm{CO}_2$ and $DIC$ variability. In the offshore subtropical region (ST) the $p\mathrm{CO}_2$ anomalies have higher amplitudes than in the adjacent continental shelf (SEBS), and are driven mainly by Temperature, with the other variables having minor contributions

345 (Fig.11). In the offshore southern region (SA), $DIC^s$ controls $p\mathrm{CO}_2$ variability, with $T$ and $ALK^s$ dampening $p\mathrm{CO}_2$ anomalies (Fig.10), similar to the adjacent shelf (PS).

    The analysis of the processes underlying this seasonal variability using our progressive sensitivity simulations shows that on all shelf regions, biological production and $\mathrm{CO}_2$ solubility mostly control

350 $p\mathrm{CO}_2$ variability (Fig.10). Physical transport, although weaker than biological production, acts to diminish the $p\mathrm{CO}_2$ variability by counteracting the effects of biology and increasing $DIC$ concentrations. In our case, physical transport controls $p\mathrm{CO}_2$ spatially, but the temporal effects of physical transport are much weaker than in Turi et al. (2014) along the California coast. This is probably because the much stronger upwelling in that region acts to dampen the effects of biology by bringing

355 $DIC$ rich waters to the surface. Along western boundaries, upwelling is weaker and more localized. Physical transport is therefore more related to processes that modulate vertical mixing and stratification, thereby controlling the seasonal enrichment of surface waters, and horizontal advection due to the presence of two major western boundary currents. Finally, air-sea $\mathrm{CO}_2$ fluxes are only a minor contribution to the $p\mathrm{CO}_2$ anomalies.

360

    In conclusion, on the Patagonia Shelf (PS), the biological production is the most important contributor to $p\mathrm{CO}_2$ variability, with a peak summer contribution of $-80$ $\mu$atm and a maximum in the winter of 70 $\mu$atm. On the South Brazilian Shelf (SBS), solubility is the most influential process (up to 90 $\mu$atm), followed by biological production and physical transport, during all seasons. On the

365 Southeast Brazilian Shelf (SEBS), the pattern is the same as in the SBS, although with a smaller magnitude and variability. Physical transport, although large in absolute contributions in the spatial analysis, has a lower contribution to $p\mathrm{CO}_2$ variability in the temporal analysis.

    In the subtropical region, processes that control the temporal variability of $p\mathrm{CO}_2$ on the shelf

370 and offshore are different. In the open ocean (ST) (Fig.11) $p\mathrm{CO}_2$ is mainly controlled by solubility, with the biological production having the least effect on $p\mathrm{CO}_2$. This contrasts with the importance of biology on mid/low latitude continental shelves (SEBS). In the subantarctic region, the processes controlling $p\mathrm{CO}_2$ are similar for both the offshore region (SA) and the adjacent continental shelf (PS) (Fig.9). In this case biological production is the most important process being countered mainly by

375 solubility, although with a smaller magnitude in the offshore region.

### 4.3 Air-sea CO$_2$ fluxes

On the continental margins, we investigate monthly averaged air-sea CO$_2$ fluxes on the inner shelf (0-100 meters depth), mid-outer shelf (100-200 meters depth) and shelf break-slope (200-1000 meters depth). As shown in the previous sections, the inner shelves have a potential to act as a source of CO$_2$, while the mid/outer shelves tend to act as a sink of CO$_2$. On the Brazilian shelves (SBS and SEBS) the flux density of CO$_2$ in the inner shelves is around $0 - 0.5$ molCm$^{-2}$yr$^{-1}$, thus ~~characterizing~~ this region as a weak source. On the mid/outer shelf ~~these regions~~ shift ~~to sinks of~~ CO$_2$, with a flux density of $-1 - 0$ molCm$^{-2}$yr$^{-1}$ on the Southeast Brazilian shelf (SEBS). On the mid/outer South Brazilian Shelf (SBS) the sink is slightly stronger with a average flux between $-1.5$ and $-0.5$ molCm$^{-2}$yr$^{-1}$ (Figs. 12a and 12b). The Patagonia Shelf (PS) acts on average as a sink of CO$_2$, with fluxes larger than on the Brazilian shelves. CO$_2$ ~~absorption on PS~~ intensifies from the inner shelf ($-1.0$ / $-0.5$ molCm$^{-2}$yr$^{-1}$) to the outer shelf and continental slope ($-2.0$ / $-4.0$ molCm$^{-2}$yr$^{-1}$) (Fig. 12c). Although, PS acts on average as a sink ~~throughout the whole continental shelf~~, there are some coastal regions that act as a source of CO$_2$, ~~which agrees~~ with the observations of Bianchi et al. (2009).

Annual mean modeled air-sea CO$_2$ fluxes agreed reasonably well with global climatologies in the oceanic regions (not shown) (Takahashi et al., 2002; Landschützer et al., 2014). South of $30°$S, the open ocean acts on average as a sink of atmospheric CO$_2$, absorbing up to $4$ molCm$^{-2}$yr$^{-1}$. North of $30°$S, the open ocean is on average in equilibrium with the atmosphere (Fig.11). On the continental margins, our annual mean air-sea CO$_2$ fluxes compare well with the global estimate from Laruelle et al. (2014), w~~here~~ the Patagonia Shelf ~~acts~~ as a sink ~~of CO$_2$~~ ($-1.0$ to $-3.0$ molCm$^{-2}$yr$^{-1}$) and the Brazilian shelves ~~act~~ as weak sources ~~of CO$_2$~~ (0 to 1 molCm$^{-2}$yr$^{-1}$). Nevertheless, we found variability ~~on each continental shelf~~, with regions on the inner Patagonia Shelf acting as a source or in equilibrium with the atmosphere (0 to 2.0 molCm$^{-2}$yr$^{-1}$), and regions on the outer Brazilian shelves acting as sinks of CO$_2$.

### 4.4 Vertical Structure - Case Study at Argentine OOI Site

Seasonal variations in mixing and stratification control the evolution of the mixed layer depth and consequently the vertical structure of the state variables of the carbonate system. Diapycnal fluxes ~~of $DIC$ and $DIC$~~ ~~sinks~~ from primary ~~production~~ are important processes regulating ocean surface $p$CO$_2$ (Rippeth et al., 2014). Therefore, ~~the mixed layer depth is linked with the~~ surface $p$CO$_2$ variability.

12

In order to understand the seasonal evolution of the upper ocean vertical distribution of the state variables in the region and how it affects surface $pCO_2$, we chose the location of the Ocean Observatory Initiative (OOI) site in the Argentine Basin at $42°$S, $42°$W (Fig.1 a), as it will soon become a test-bed for the validation of biogeochemical models globally and regionally. We extracted modeled climatological vertical profiles of $DIC$ concentration, temperature and chlorophyll-a, and compared with the modeled surface $pCO_2$ and mixed layer depth (Fig.13).

During the entire year, this location acts in our model as a sink for atmospheric $CO_2$, with modeled surface $pCO_2$ ranging from 280 $\mu$atm to 320 $\mu$atm. The contribution of $DIC^s$ and $T$ are again driving surface $pCO_2$ anomalies. In this case $DIC^s$ is controlling the anomalies signal, being ~~dampened~~ by temperature. The main processes affecting $pCO_2$ in this location is biological production and solubility. Minimum $pCO_2$ in summer coincides with strong stratification and elevated subsurface biological production, respectively, with the opposing contribution of $DIC^s$ and $T$ leading to $pCO_2$ anomalies near zero. Maximum $pCO_2$ occurs when the mixed layer depth deepens, during fall and winter, ~~when vertical mixing cause~~ an increase in ~~the~~ concentration ~~of $DIC$~~ in ~~the~~ surface waters. This ~~affects~~ $pCO_2$ ~~much more~~ than the decrease in temperature, resulting in positive $pCO_2$ anomalies. ~~After winter, this~~ excess of $DIC$ is consumed by biological fixation during spring and summer, thus reducing surface $pCO_2$.

## 5  Conclusions

In this study, we used a regional hydrodynamic model coupled to a biogeochemical model to investigate, ~~in a climatological sense~~, the main parameters and processes that control ocean surface $pCO_2$ and air-sea $CO_2$ fluxes in the southwestern Atlantic Ocean. Modeled ocean surface $pCO_2$ compared well with the available in-situ data, reproducing the expected meridional and cross-shelf gradients of $pCO_2$, with elevated $pCO_2$ in the inner shelves and at lower latitudes. Our results highlight that the most important variables controlling the spatio-temporal variability of $pCO_2$ are $T$ and $DIC^s$. These two variables have opposing effects on $pCO_2$ and have been shown to be the main drivers of $pCO_2$ both in global (Sarmiento and Gruber, 2006; Doney et al., 2009) and in other regional studies (Turi et al., 2014; Signorini et al., 2013; Lovenduski et al., 2007). ~~Following $DIC^s$ and $T$, we found that~~ $ALK^s$ is ~~a secondarily important~~ spatial regulator of $pCO_2$, with ~~increasing importance on~~ the South brazilian Shelf (SBS) and in the southern open ocean region (SA).

The most important processes underlying changes on the state variables and thus on $pCO_2$ are biological production and $CO_2$ solubility. Biological production is particularly important on the continental shelves , with higher contribution ~~in shelf regions~~ at high latitudes. In the open ocean,

CO$_2$ solubility is the main process driving $p$CO$_2$ variations in the subtropics, while in the subantarctic both CO$_2$ solubility and biological production are important drivers of $p$CO$_2$ variability.

The southwestern Atlantic Ocean acts, on average, as a sink of atmospheric CO$_2$ south of 30°S, and is close to equilibrium to the north. In the inner continental shelves the ocean acts either as a weak source or is in equilibrium with the atmosphere. To the outer shelf the ocean ~~changes~~ to a sink of CO$_2$. The entire Patagonian shelf act, on average, as a sink, but there are some particular regions in the inner shelf that act~~s~~ as a source of CO$_2$. The total integrated flux agrees well with Laruelle et al. (2014), particularly on the Brazilian Shelves (SEBS and SBS). ~~However, in~~ the Patagonia Shelf (PS), we found a slightly stronger sink on the mid/outer Patagonian Shelf ($-1.0$ to $-3.0$ molCm$^{-2}$yr$^{-1}$) and more variability towards the inner shelf.

Our model does not include river inputs of carbon, which are known to be an important factor regulating $p$CO$_2$ (Bauer et al., 2013). The lack of tides may adversely affect our model results in the inner shelf of Patagonia, where tidal amplitudes reach up to 12 meters ~~at some points~~ (Kantha, 1995; Saraceno et al., 2010) and tidal fronts are known to impact oceanic $p$CO$_2$ (Bianchi et al., 2005). In future regional studies focused on the Patagonia shelf, tides and river run-off should be included.

Modeling studies such as this one depend heavily on in-situ observations, the lack of which hampers our ability to properly refine our model. This will certainly be improved by future efforts ~~of~~ data assimilation ~~of~~ vertical profiles of biogeochemical and physical variables ~~from~~ the OOI site ~~at~~ the Argentine basin. This study is a first step ~~in~~ understanding the processes controlling surface $p$CO$_2$ in an undersampled, yet highly important, region of the world's ocean. ~~Improved understanding of the processes controlling the surface distribution of $p$CO$_2$ on continental shelves and in the open ocean is fundamental for quantifying the ocean's response to and its feedback on climate change.~~

**Appendix A: Model Validation (SST and Chlorophyll-a)**

Seasonal climatologies of 4 years of modeled sea surface temperature and chlorophyll-a concentration were compared with climatologies from the sensors AVHRR (1985-2002) and Modis-aqua (2003-2013), respectively (Figs. 14 and 15). Modeled sea surface temperature compared well with AVHRR (Fig.14) representing both subantarctic and subtropical oceanic regions during all seasons.

Modeled chlorophyll-a concentration reproduces the general pattern from MODIS-aqua (Fig.15), with low concentrations in the oceanic regions and higher concentrations on the continental shelves. However, modeled chlorophyll-a concentrations are overestimated in the open ocean regions (0.5

mgChla-am$^{-3}$), especially in the spring season (up to 1 mgChla-am$^{-3}$). In the coastal regions, we underestimate chlorophyll-a on the Patagonia Shelf during spring and summer seasons. Expectedly, there was an underestimation in the La Plata region, since we are not modeling the nutrient and organic loads from the river. Finally, on the Brazilian shelf our model overestimates chlorophyll-a, particularly during summer and spring seasons. These biases may be due to our application of a relatively simple ecosystem model with only one phytoplankton functional type in such a wide region, which encompasses several ecological provinces. Nevertheless, the general pattern is well reproduced in this first effort in modeling the biogeochemistry of the southwestern Atlantic Ocean, and the biases may not significantly compromise our analysis of drivers and processes of $p$CO$_2$ variability.

## References

Allen, J., Somerfield, P., and Gilbert, F.: Quantifying uncertainty in high-resolution coupled hydrodynamic-ecosystem models, Journal of Marine Systems, 64, 3–14, doi:10.1016/j.jmarsys.2006.02.010, http://linkinghub.elsevier.com/retrieve/pii/S0924796306001035, 2007.

Bakker, D. C. E., Pfeil, B., Smith, K., Hankin, S., Olsen, a., Alin, S. R., Cosca, C., Harasawa, S., Kozyr, a., Nojiri, Y., O'Brien, K. M., Schuster, U., Telszewski, M., Tilbrook, B., Wada, C., Akl, J., Barbero, L., Bates, N., Boutin, J., Cai, W.-J., Castle, R. D., Chavez, F. P., Chen, L., Chierici, M., Currie, K., de Baar, H. J. W., Evans, W., Feely, R. a., Fransson, a., Gao, Z., Hales, B., Hardman-Mountford, N., Hoppema, M., Huang, W.-J., Hunt, C. W., Huss, B., Ichikawa, T., Johannessen, T., Jones, E. M., Jones, S. D., Jutterström, S., Kitidis, V., Körtzinger, a., Landschtzer, P., Lauvset, S. K., Lefèvre, N., Manke, a. B., Mathis, J. T., Merlivat, L., Metzl, N., Murata, a., Newberger, T., Ono, T., Park, G.-H., Paterson, K., Pierrot, D., Ríos, a. F., Sabine, C. L., Saito, S., Salisbury, J., Sarma, V. V. S. S., Schlitzer, R., Sieger, R., Skjelvan, I., Steinhoff, T., Sullivan, K., Sun, H., Sutton, a. J., Suzuki, T., Sweeney, C., Takahashi, T., Tjiputra, J., Tsurushima, N., van Heuven, S. M. a. C., Vandemark, D., Vlahos, P., Wallace, D. W. R., Wanninkhof, R., and Watson, a. J.: An update to the Surface Ocean $CO_2$ Atlas (SOCAT version 2), Earth System Science Data Discussions, 6, 465–512, doi:10.5194/essdd-6-465-2013, http://www.earth-syst-sci-data-discuss.net/6/465/2013/, 2013.

Bauer, J. E., Cai, W.-J., Raymond, P. a., Bianchi, T. S., Hopkinson, C. S., and Regnier, P. a. G.: The changing carbon cycle of the coastal ocean., Nature, 504, 61–70, doi:10.1038/nature12857, http://www.ncbi.nlm.nih.gov/pubmed/24305149, 2013.

Bianchi, A. A., Piola, A. R., Pino, D. R., Schloss, I., Poisson, A., and Balestrini, C. F.: Vertical stratification and air-sea CO 2 fluxes in the Patagonian shelf, Journal of Geophysical Research, 110, C07 003, doi:10.1029/2004JC002488, http://doi.wiley.com/10.1029/2004JC002488, 2005.

Bianchi, A. a., Pino, D. R., Perlender, H. G. I., Osiroff, A. P., Segura, V., Lutz, V., Clara, M. L., Balestrini, C. F., and Piola, A. R.: Annual balance and seasonal variability of sea-air CO 2 fluxes in the Patagonia Sea: Their relationship with fronts and chlorophyll distribution, Journal of Geophysical Research, 114, C03 018, doi:10.1029/2008JC004854, http://doi.wiley.com/10.1029/2008JC004854, 2009.

Cai, W.-J.: The role of marsh-dominated heterotrophic continental margins in transport of CO 2 between the atmosphere, the land-sea interface and the ocean, Geophysical Research Letters, 30, 1849, doi:10.1029/2003GL017633, http://doi.wiley.com/10.1029/2003GL017633, 2003.

Carton, J. A. and Giese, B. S.: A reanalysis of ocean climate using Simple Ocean Data Assimilation (SODA), Monthly Weather Review, 136, 2999–3017, 2008.

Chen, C.-T. a., Huang, T.-H., Chen, Y.-C., Bai, Y., He, X., and Kang, Y.: Air-sea exchanges of $CO_2$ in world's coastal seas, Biogeosciences Discussions, 10, 5041–5105, doi:10.5194/bgd-10-5041-2013, http://www.biogeosciences-discuss.net/10/5041/2013/, 2013.

Ciais, P., Sabine, C., Bala, G., Bopp, L., Brovkin, V., Canadell, J., Chhabra, A., DeFries, R., Galloway, J., Heimann, M., et al.: Carbon and other biogeochemical cycles, in: Climate Change 2013: The Physical Science Basis. Contribution of Working Group I to the Fifth Assessment Report of the Intergovernmental Panel on Climate Change, pp. 465–570, Cambridge University Press, 2014.

Da Silva, A., Young, C., and Levitus, S.: Atlas of surface marine data 1994, vol. 1, algorithms and procedures, NOAA Atlas NESDIS 6, US Department of Commerce, NOAA, NESDIS, USA, p. 74, 1994.

555 Dabrowski, T., Lyons, K., Berry, A., Cusack, C., and Nolan, G. D.: An operational biogeochemical model of the North-East Atlantic: Model description and skill assessment, Journal of Marine Systems, 129, 350–367, doi:10.1016/j.jmarsys.2013.08.001, http://linkinghub.elsevier.com/retrieve/pii/S0924796313001711, 2014.

Doney, S. C., Lima, I., Feely, R. a., Glover, D. M., Lindsay, K., Mahowald, N., Moore, J. K., and Wanninkhof, R.: Mechanisms governing interannual variability in upper-ocean inorganic carbon system and
560 air–sea CO2 fluxes: Physical climate and atmospheric dust, Deep Sea Research Part II: Topical Studies in Oceanography, 56, 640–655, doi:10.1016/j.dsr2.2008.12.006, http://linkinghub.elsevier.com/retrieve/pii/S096706450800427X, 2009.

Fennel, K. and Wilkin, J.: Quantifying biological carbon export for the northwest North Atlantic continental shelves, Geophysical Research Letters, 36, 2009.

565 Gonzalez-Silvera, A., Santamaria-del Angela, E., Garcia, V. M. T., Garcia, C. A. E., Millan-Nunez, R., and Muller-Karger, F.: Biogeographical regions of the tropical and subtropical Atlantic Ocean off South America: classification based on pigment (CZCS) and chlorophyll- a(SeaWiFS), Continental Shelf . . . , 24, 983–1000, doi:10.1016/j.csr.2004.03.002, http://www.sciencedirect.com/science/article/pii/S0278434304000561, 2004.

570 Gruber, N.: Ocean biogeochemistry: Carbon at the coastal interface, Nature, 2015.

Gruber, N., Frenzel, H., Doney, S. C., Marchesiello, P., McWilliams, J. C., Moisan, J. R., Oram, J. J., Plattner, G.-K., and Stolzenbach, K. D.: Eddy-resolving simulation of plankton ecosystem dynamics in the California Current System, Deep Sea Research Part I: Oceanographic Research Papers, 53, 1483–1516, doi:10.1016/j.dsr.2006.06.005, http://linkinghub.elsevier.com/retrieve/pii/S0967063706001713, 2006.

575 Gruber, N., Lachkar, Z., Frenzel, H., Marchesiello, P., Münnich, M., McWilliams, J. C., Nagai, T., and Plattner, G.-K.: Eddy-induced reduction of biological production in eastern boundary upwelling systems, Nature Geoscience, 4, 787–792, doi:10.1038/ngeo1273, http://www.nature.com/doifinder/10.1038/ngeo1273, 2011.

Guerrero, R. A., Piola, A. R., Fenco, H., Matano, R. P., Combes, V., Chao, Y., James, C., Palma, E. D., Saraceno, M., and Strub, P. T.: The salinity signature of the cross-shelf exchanges in the Southwestern Atlantic Ocean:
580 Satellite observations, Journal of Geophysical Research: Oceans, 119, 7794–7810, 2014.

Hauri, C., Gruber, N., Vogt, M., Doney, S. C., Feely, R. A., Lachkar, Z., Leinweber, A., McDonnell, A. M., Munnich, M., and Plattner, G.-K.: Spatiotemporal variability and long-term trends of ocean acidification in the California Current System, 2013.

Hofmann, E. E., Cahill, B., Fennel, K., a.M. Friedrichs, M., Hyde, K., Lee, C., Mannino, A., Najjar, R. G.,
585 O'Reilly, J. E., Wilkin, J., and Xue, J.: Modeling the Dynamics of Continental Shelf Carbon, Annual Review of Marine Science, 3, 93–122, doi:10.1146/annurev-marine-120709-142740, http://www.annualreviews.org/doi/abs/10.1146/annurev-marine-120709-142740, 2011.

Ito, R., Schneider, B., and Thomas, H.: Distribution of surface fCO2 and air–sea fluxes in the Southwestern subtropical Atlantic and adjacent continental shelf, Journal of Marine Systems, 56, 227–242,
590 doi:10.1016/j.jmarsys.2005.02.005, http://linkinghub.elsevier.com/retrieve/pii/S0924796305000436, 2005.

Kantha, L.: Barotropic tides in the global oceans from a nonlinear tidal model assimilating altimetric tides: 1. Model description and results, Journal of Geophysical Research: Oceans (1978– . . . , 100, 283–308, http://onlinelibrary.wiley.com/doi/10.1029/95JC02578/full, 1995.

17

Körtzinger, A.: Determination of carbon dioxide partial pressure (p (CO2)), Methods of Seawater Analysis, Third Edition, pp. 149–158, 1999.

Landschützer, P., Gruber, N., Bakker, D., and Schuster, U.: Recent variability of the global ocean carbon sink, Global Biogeochemical Cycles, 28, 927–949, 2014.

Laruelle, G. G., Dürr, H. H., Lauerwald, R., Hartmann, J., Slomp, C. P., Goossens, N., and Regnier, P. a. G.: Global multi-scale segmentation of continental and coastal waters from the watersheds to the continental margins, Hydrology and Earth System Sciences, 17, 2029–2051, doi:10.5194/hess-17-2029-2013, http://www.hydrol-earth-syst-sci.net/17/2029/2013/, 2013.

Laruelle, G. G., Lauerwald, R., Pfeil, B., and Regnier, P.: Regionalized global budget of the CO2 exchange at the air-water interface in continental shelf seas, Global biogeochemical cycles, 28, 1199–1214, 2014.

Lovenduski, N. S., Gruber, N., Doney, S. C., and Lima, I. D.: Enhanced CO 2 outgassing in the Southern Ocean from a positive phase of the Southern Annular Mode, Global Biogeochemical Cycles, 21, n/a–n/a, doi:10.1029/2006GB002900, http://doi.wiley.com/10.1029/2006GB002900, 2007.

Millero, F.: Thermodynamics of the carbon dioxide system in the oceans, Geochimica et Cosmochimica Acta, 59, 661–677, http://www.sciencedirect.com/science/article/pii/001670379400354O, 1995.

Moore, J. K., Lindsay, K., Doney, S. C., Long, M. C., and Misumi, K.: Marine ecosystem dynamics and biogeochemical cycling in the Community Earth System Model [CESM1 (BGC)]: Comparison of the 1990s with the 2090s under the RCP4. 5 and RCP8. 5 scenarios, Journal of Climate, 26, 9291–9312, 2013.

Muller-Karger, F. E., Varela, R., Thunell, R., Luerssen, R., Hu, C., and Walsh, J. J.: The importance of continental margins in the global carbon cycle, Geophysical Research Letters, 32, 2005.

Nash, J. and Sutcliffe, J.: River flow forecasting through conceptual models part I—A discussion of principles, Journal of hydrology, 10, 282–290, 1970.

Ospar, V. M., De Vries, I., Bokhorst, M., Ferreira, J., Gellers-Barkmann, S., Kelly-Gerreyn, B., Lancelot, C., Mensguen, A., Moll, A., Pätsch, J., Radach, G., Skogen, M., Soiland, H., Svendsen, E., and Vested, H. J.: Report of the ASMO modelling workshop on eutrophication Issues, 5–8 November 1996, OSPAR Commission Report, 102, 90, 1998.

Piola, A. and Matano, R.: Brazil and Falklands (Malvinas) currents, Ocean Currents: A Derivative of the Encyclopedia of Ocean Sciences, pp. 35–43, 2001.

Rippeth, T., Lincoln, B., Kennedy, H., Palmer, M., Sharples, J., and Williams, C.: Impact of vertical mixing on sea surface pCO2 in temperate seasonally stratified shelf seas, Journal of Geophysical Research: Oceans, 119, 3868–3882, 2014.

Risien, C. M. and Chelton, D. B.: A global climatology of surface wind and wind stress fields from eight years of QuikSCAT scatterometer data, Journal of Physical Oceanography, 38, 2379–2413, 2008.

Saraceno, M., D'Onofrio, E., Fiore, M., and Grismeyer, W.: Tide model comparison over the Southwestern Atlantic Shelf, Continental Shelf Research, 30, 1865–1875, doi:10.1016/j.csr.2010.08.014, http://linkinghub.elsevier.com/retrieve/pii/S0278434310002712, 2010.

Sarmiento, J. and Gruber, N.: Ocean biogeochemical dynamics, Princeton University Press, 2006.

Shchepetkin, A. and McWilliams, J.: The regional oceanic modeling system (ROMS): a split-explicit, free-surface, topography-following-coordinate oceanic model, Ocean Modelling, 9, 347–404, http://linkinghub.elsevier.com/retrieve/pii/S1463500304000484, 2005.

Signorini, S. R., Mannino, A., Najjar, R. G., Friedrichs, M. a. M., Cai, W.-J., Salisbury, J., Wang, Z. A., Thomas, H., and Shadwick, E.: Surface ocean p CO 2 seasonality and sea-air CO 2 flux estimates for the North American east coast, Journal of Geophysical Research: Oceans, 118, 5439–5460, doi:10.1002/jgrc.20369, http://doi.wiley.com/10.1002/jgrc.20369, 2013.

Stow, C. A., Jolliff, J., McGillicuddy, D. J., Doney, S. C., Allen, J. I., Friedrichs, M. A., Rose, K. A., and Wallhead, P.: Skill assessment for coupled biological/physical models of marine systems, Journal of Marine Systems, 76, 4–15, 2009.

Takahashi, T., Sutherland, S. C., Sweeney, C., Poisson, A., Metzl, N., Tilbrook, B., Bates, N., Wanninkhof, R., Feely, R. A., Sabine, C., Olafsson, J., and Nojiri, Y.: Global sea–air CO 2 flux based on climatological surface ocean p CO 2 , and seasonal biological and temperature effects, Deep Sea Research Part II: Topical Studies in Oceanography, 49, 1601–1622, 2002.

Takahashi, T., Sutherland, S. C., Wanninkhof, R., Sweeney, C., Feely, R. A., Chipman, D. W., Hales, B., Friederich, G., Chavez, F., Sabine, C., et al.: Climatological mean and decadal change in surface ocean pCO 2, and net sea–air CO 2 flux over the global oceans, Deep Sea Research Part II: Topical Studies in Oceanography, 56, 554–577, 2009.

Tsunogai, S., Watanabe, S., and Sato, T.: Is there a "continental shelf pump" for the absorption of atmospheric CO2?, Tellus B, 51B, 701–712, http://onlinelibrary.wiley.com/doi/10.1034/j.1600-0889.1999.t01-2-00010.x/abstract, 1999.

Turi, G., Lachkar, Z., and Gruber, N.: Spatiotemporal variability and drivers of $CO_2$ and air–sea $CO_2$ fluxes in the California Current System: an eddy-resolving modeling study, Biogeosciences, 11, 671–690, doi:10.5194/bg-11-671-2014, http://www.biogeosciences.net/11/671/2014/, 2014.

Walsh, J.: Importance of continental margins in the marine biogeochemical cycling of carbon and nitrogen, Nature, 350, 53–55, http://www.ccpo.odu.edu/~klinck/Reprints/PDF/walshNature91.pdf, 1991.

Wang, A. Z., Cai, W.-J., Wang, Y., and Ji, H.: The southeastern continental shelf of the United States as an atmospheric CO2 source and an exporter of inorganic carbon to the ocean, Continental Shelf Research, 25, 1917–1941, doi:10.1016/j.csr.2005.04.004, http://linkinghub.elsevier.com/retrieve/pii/S0278434305000774, 2005.

Yool, A. and Fasham, M.: An examination of the "continental shelf pump" in an open ocean general circulation model, Global Biogeochemical Cycles, 15, 831–844, http://onlinelibrary.wiley.com/doi/10.1029/2000GB001359/full, 2001.
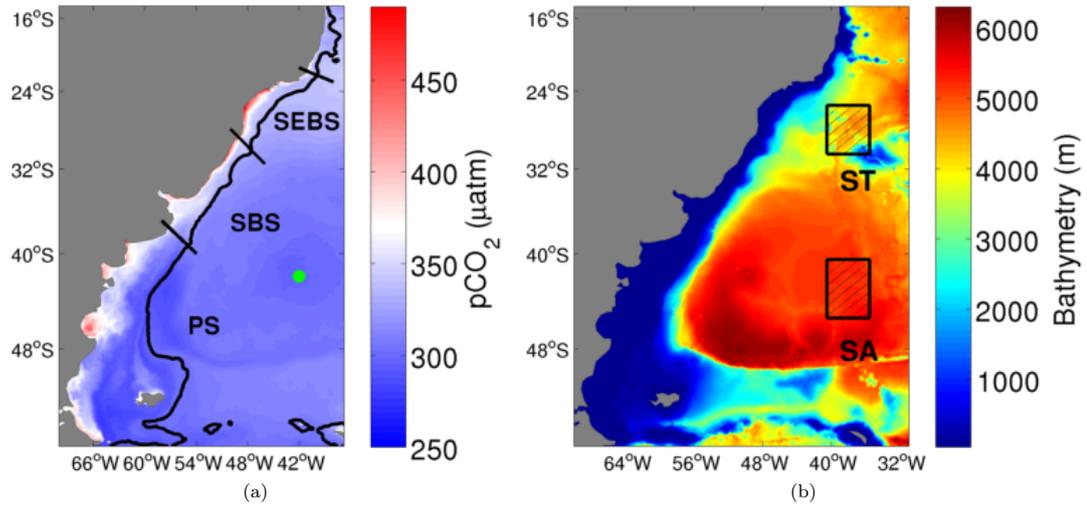
**Figure 1.** Areas utilised for the temporal analysis, (a) show the 3 continental shelves (SEBS, SBS and PS) analysed in a map with annual mean ocean surface $p\mathrm{CO_2}$. The green circle represents the location of the vertical profile at the OOI site. (b) show the two oceanic regions (ST and SA) in a map with bathymetry.

**Table 1.** Statistical indicators of model skill for surface ocean $p\mathrm{CO_2}$ in the three areas (A1, A2 and A3 - Fig.4). The indicators are: ME (Model Efficiency); CF (Cost Function); and PB (Percentage of Bias). Additionally, showing total bias ($\mu$atm), correlation and total number of observations (N) available on each area. Bold values indicate "good/reasonable" model skill.

| Area | ME | CF | PB | Bias | Correlation | N |
|------|------|------|-------|-------|-------------|----|
| A1 | **0.23** | **0.52** | **2.88** | 10.26 | 0.80 | 77 |
| A2 | −0.18 | **0.61** | **4.23** | 15.0 | −0.34 | 60 |
| A3 | −4.70 | **1.83** | **11.59** | 40.4 | −0.13 | 40 |
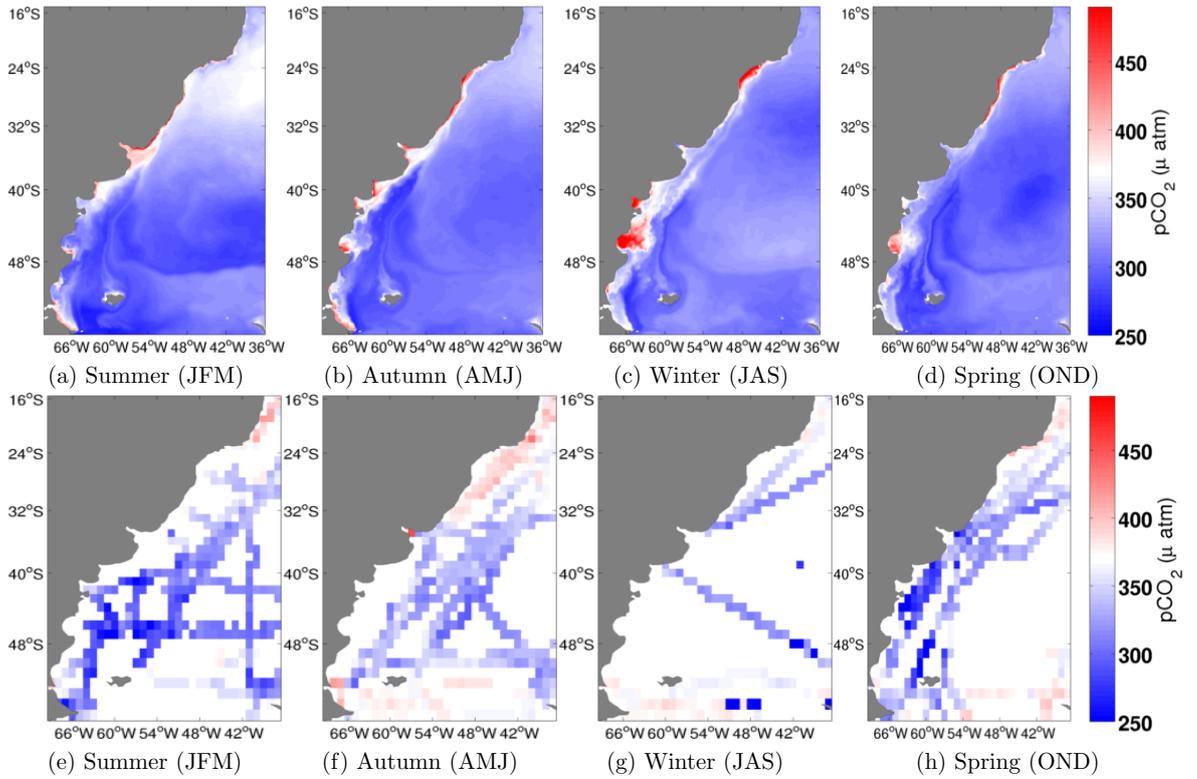
**Figure 2.** Seasonal climatology of modeled ocean surface $p\text{CO}_2$ (upper row) and observations of $p\text{CO}_2$ from the SOCAT database (lower row). The white separation between red and blue is set to 370 $\mu$atm which is the atmospheric $p\text{CO}_2$ used in this study. Blue represents a sink of atmospheric $\text{CO}_2$ and red a source.

21
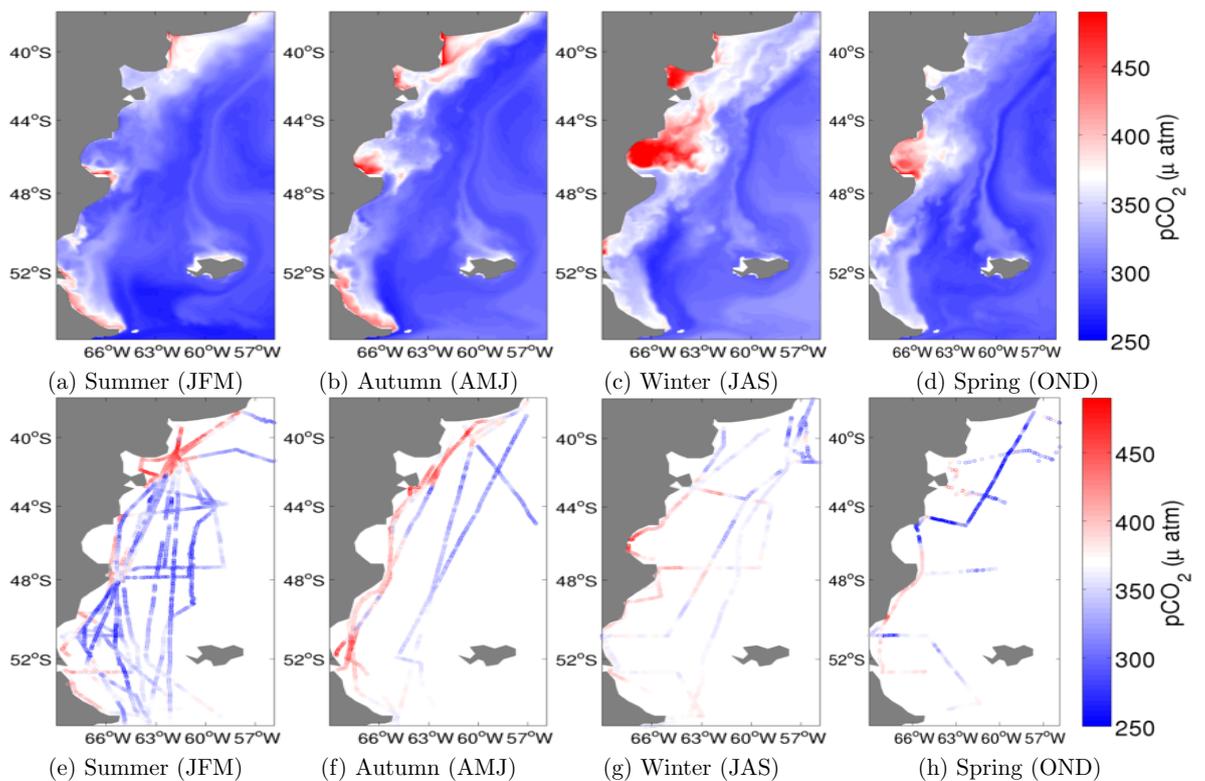
**Figure 3.** Model evaluation on the Patagonia Shelf (PS) (zoom in from model domain in Fig. 2a). Seasonal climatology of modeled ocean surface $pCO_2$ (upper row) and $pCO_2$ observations from ARGAU and GEF3 cruises(lower row) (Bianchi et al., 2009). The white separation between red and blue is set to 370 $\mu$atm which is the atmospheric $pCO_2$ used in this study. Blue represents a sink of atmospheric $CO_2$ and red a source.
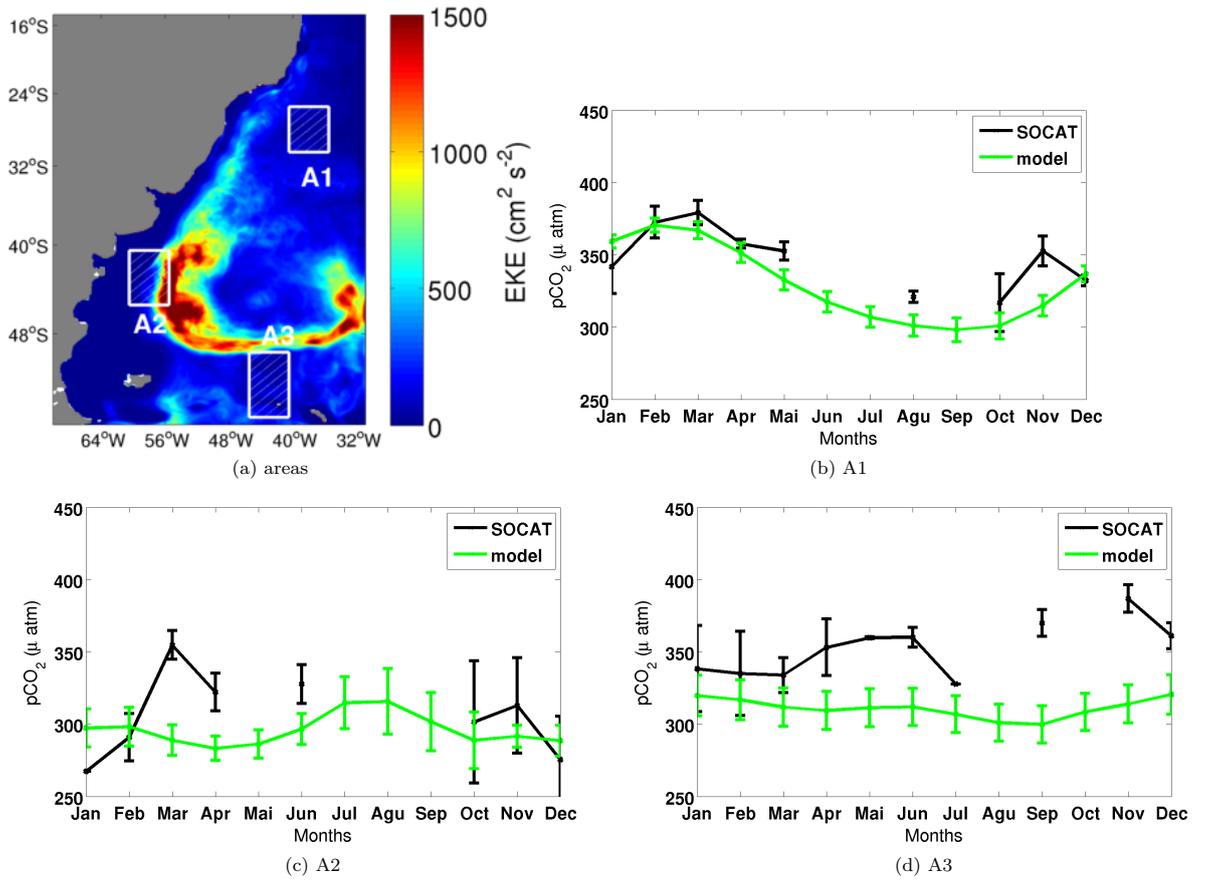
**Figure 4.** Location of the three areas used for the monthly comparison with SOCAT database (a) in a map with annual mean eddy kinetic energy. In figures (b), (c) and (d), green lines are the modeled monthly mean $p\text{CO}_2$ and black lines are the monthly mean $p\text{CO}_2$ from SOCAT. Error bars are two standard deviations
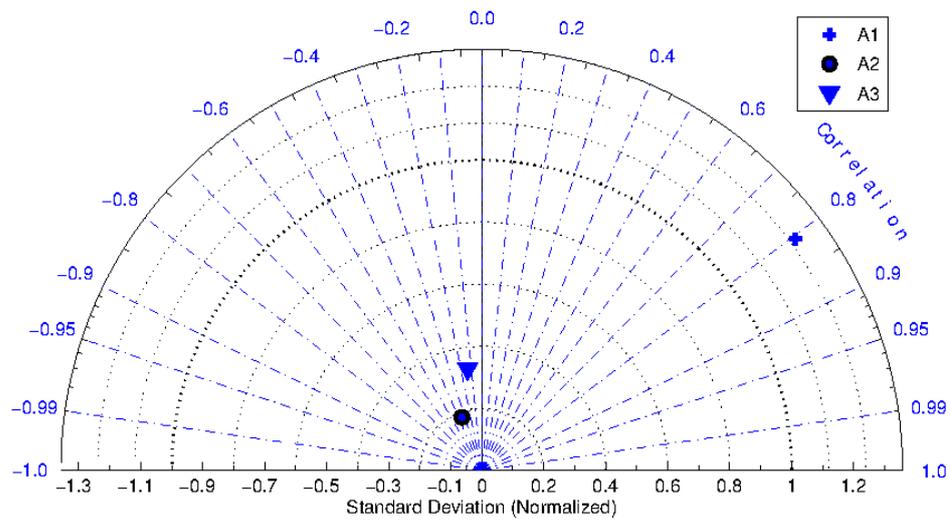
**Figure 5.** Taylor Diagram showing the three areas used for comparison with SOCAT observational data. A1 is the only area with statistically significant correlation.

(a) pCO2 Anomalies

(b) $\frac{\partial pCO_2}{\partial ALK}\Delta ALK^s$     (c) $\frac{\partial pCO_2}{\partial FW}\Delta FW$     (d) $\frac{\partial pCO_2}{\partial T}\Delta T$     (e) $\frac{\partial pCO_2}{\partial DIC}\Delta DIC^s$
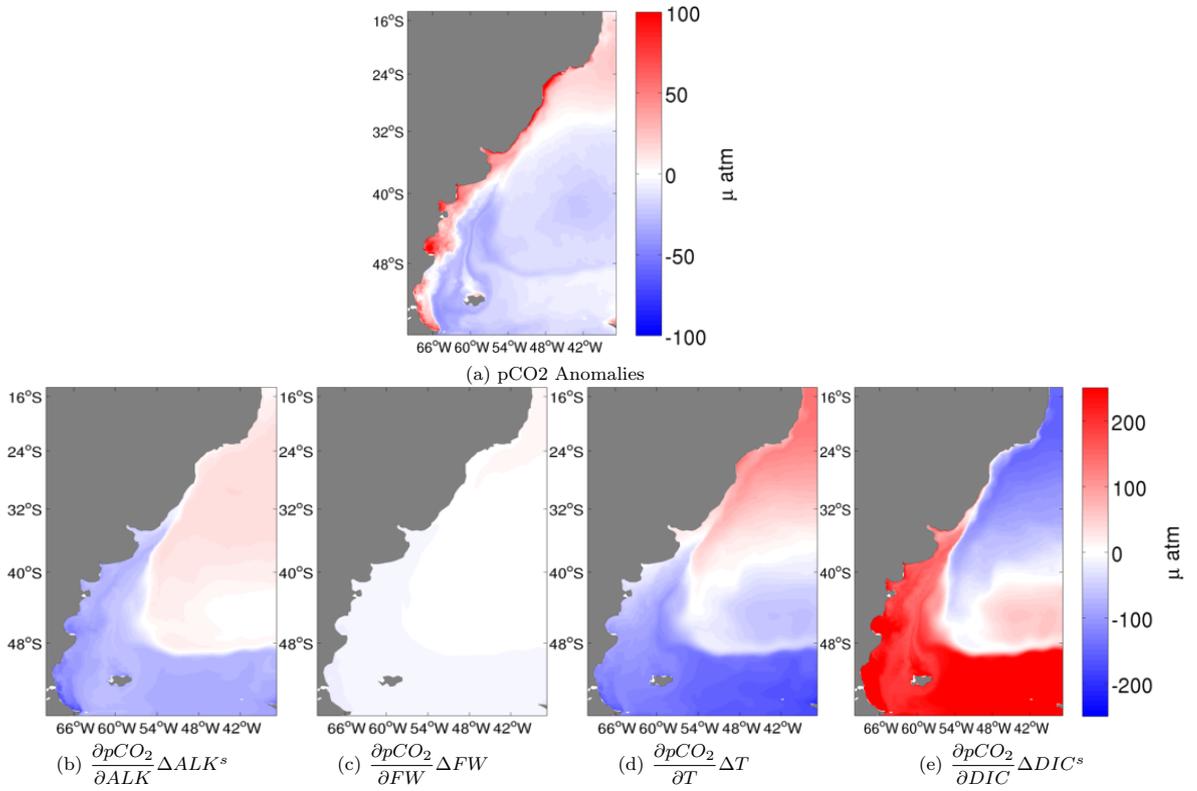
**Figure 6.** $p$CO$_2$ spatial anomalies - difference between annual mean and domain mean (a) and the contribution of the main drivers: $ALK^s$ (b), FW (c), $T$ (d) and $DIC^s$ (e). Computed using spatial anomalies for $\Delta$
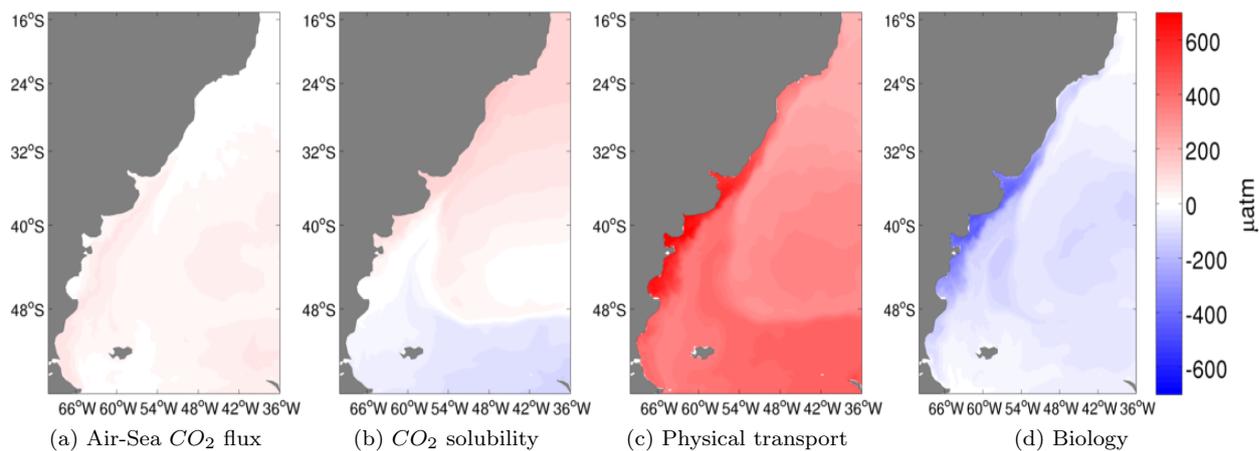
**Figure 7.** Processes driving the annual mean surface $p$CO$_2$. Contribution of Air-sea flux of CO$_2$ [Control - E1] (a), CO$_2$ solubility [E2 - E3] (b), physical transport [E3] (c) and biological production [E1 - E2] (d)
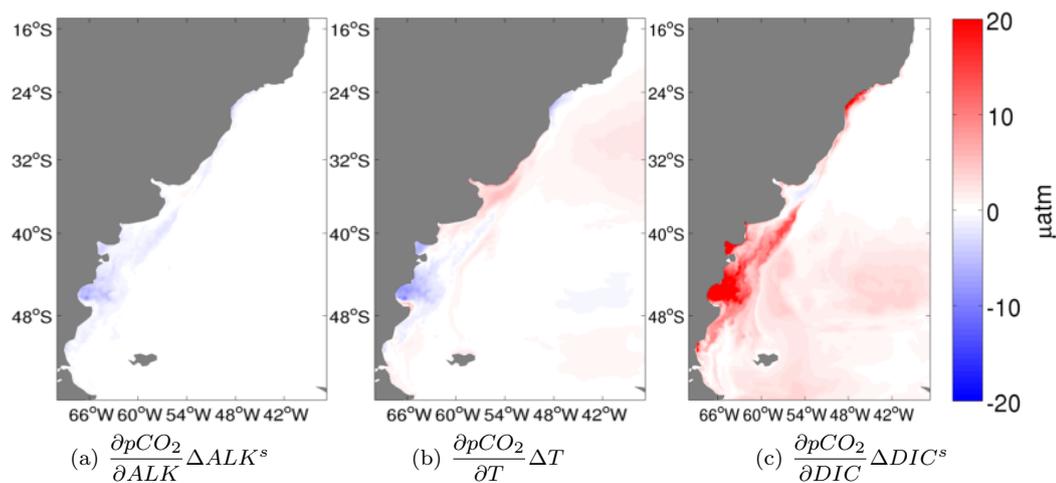


**Figure 8.** Sensitivity of $p$CO$_2$ computed with grid point anomalies in time to local annual means. Annual mean contribution of the main drivers: $ALK^s$ (a), $T$ (b) and $DIC^s$ (c).

(a) PS

(b) SBS

(c) SEBS
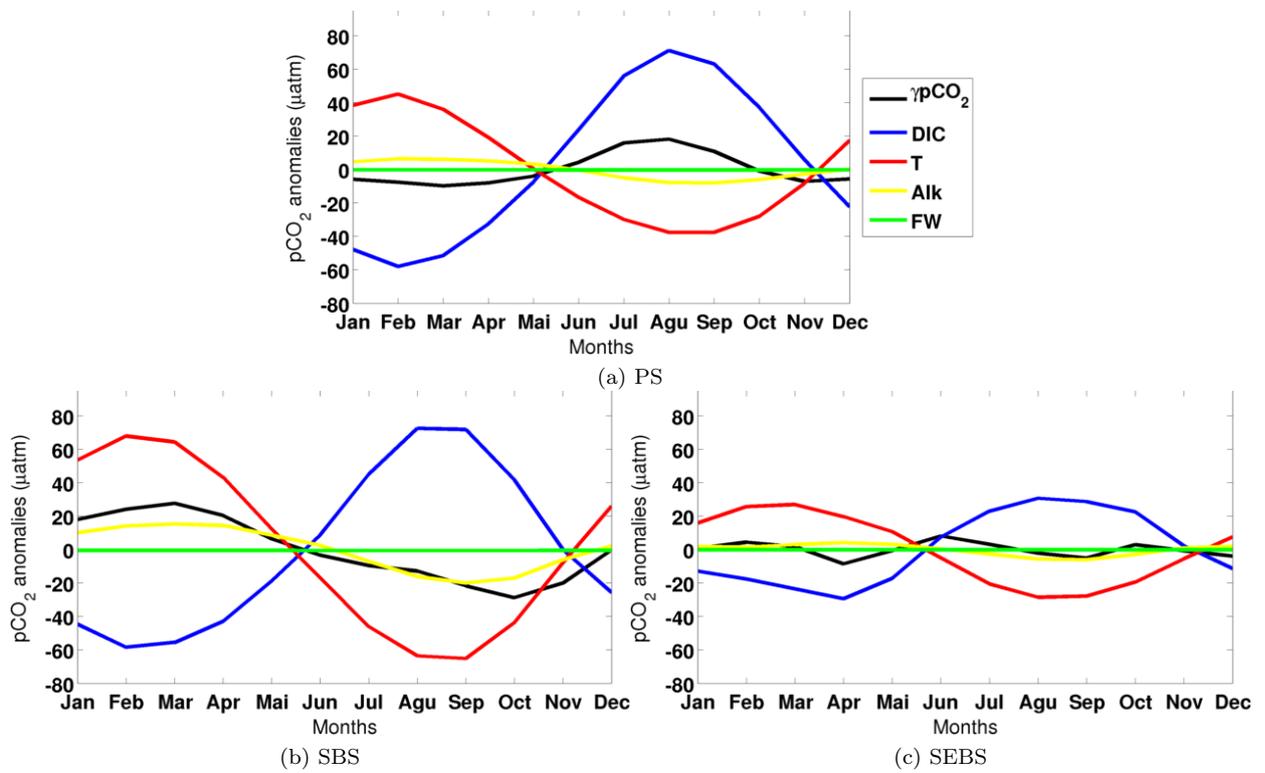
**Figure 9.** Temporal evolution of $p$CO$_2$ anomalies and their drivers in each continental shelf (right hand side of Eq. 1 using temporal anomalies), red line represents the effects of Temperature, blue line the effects of $DIC^s$, green line FW, and yellow line $ALK^s$.

(a) PS

(b) SBS

(c) SEBS
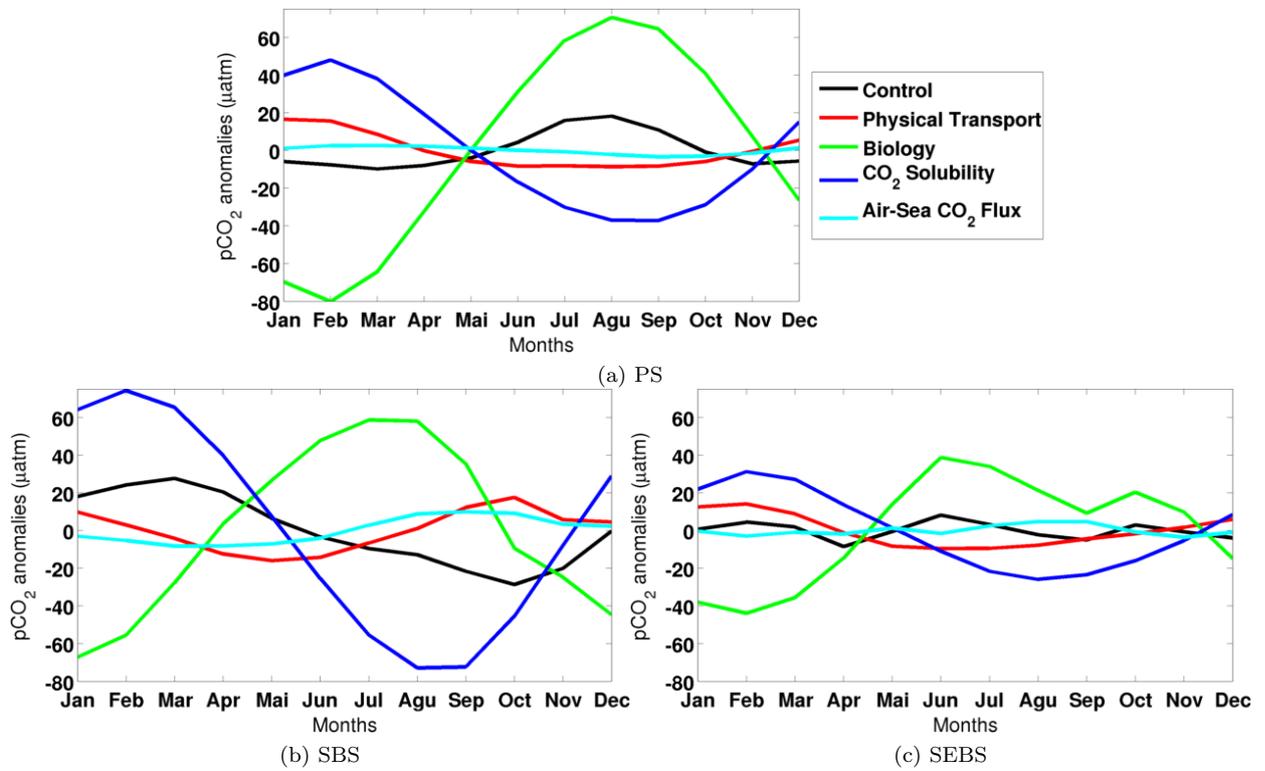
**Figure 10.** temporal evolution of the monthly anomalies of each process in regulating $pCO_2$ anomalies, green line represents the biological production, red line the physical transport, light blue line the air-sea $CO_2$ fluxes and dark blue line the solubility. Black lines represent the temporal $pCO_2$ anomalies.
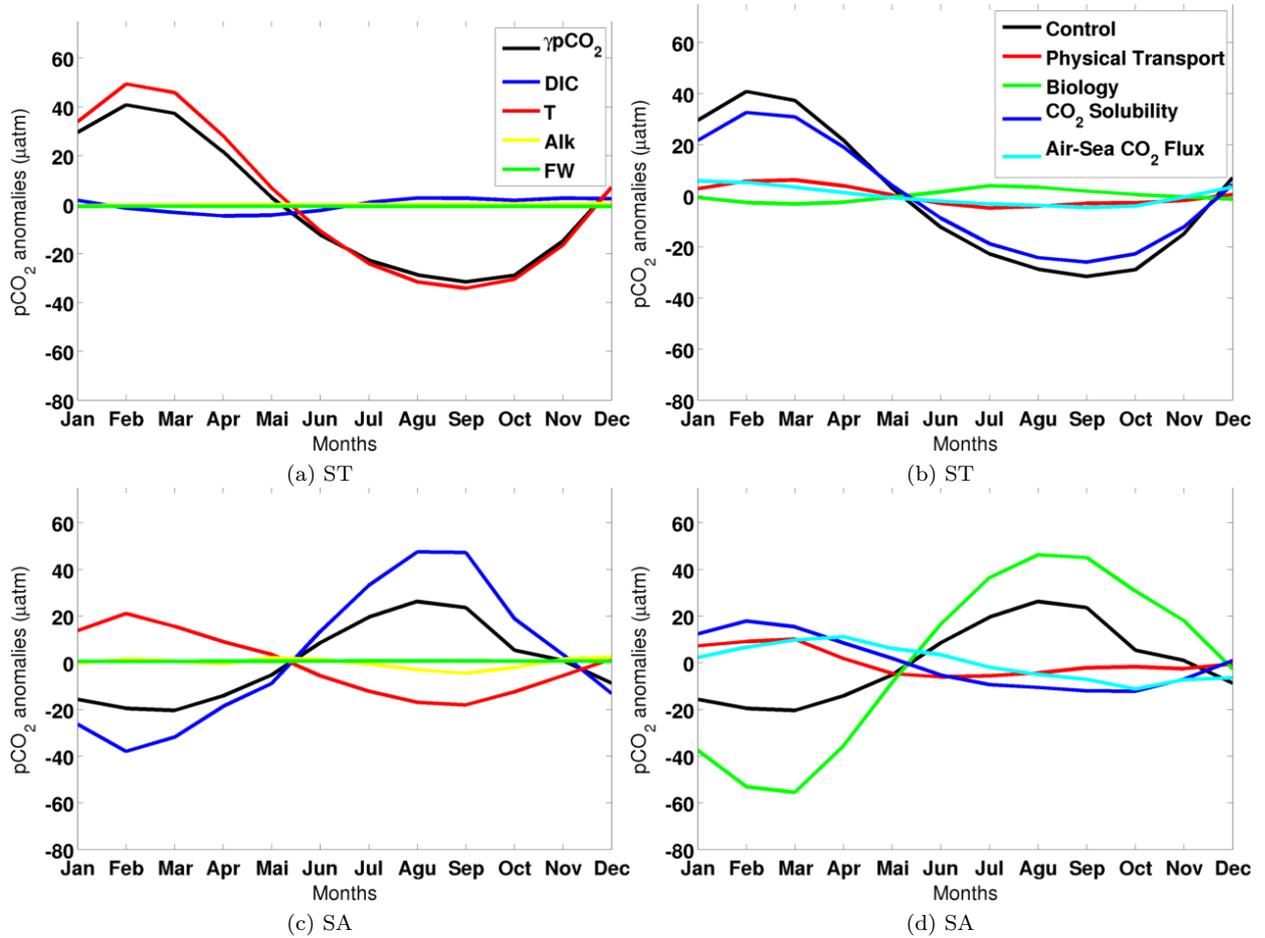
**Figure 11.** Figures (a) and (b) show the temporal evolution of $p$CO$_2$ anomalies and its drivers in each oceanic regions (ST and SA) (right hand side of Eq. 1 using temporal anomalies), red line represents the effects of $T$, blue line the effects of $DIC^s$, green line the FW and yellow line $ALK^s$. Figures (c), and (e) show the temporal evolution of the monthly anomalies of each process in regulating temporal $p$CO$_2$ anomalies, green line represents the biological production, red line the physical transport, light blue line the air-sea CO$_2$ fluxes and dark blue line the solubility. Black lines represent the temporal $p$CO$_2$ anomalies.
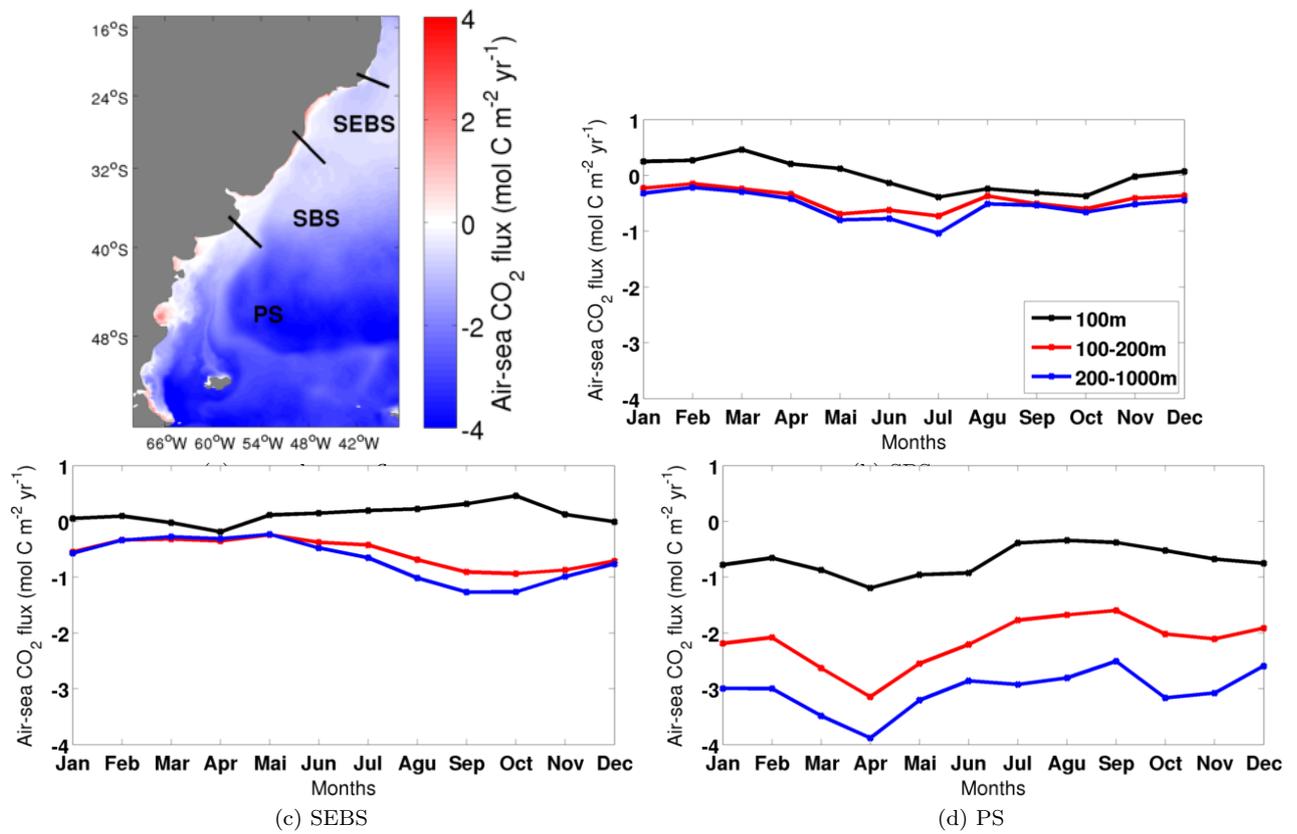
**Figure 12.** Figure (a) is the annual mean of air-sea $CO_2$ fluxes. Figures (b), (c) and (d) show the monthly average of surface $CO_2$ fluxes constrained to bathymetry levels of 100m, 200m and 1000m.
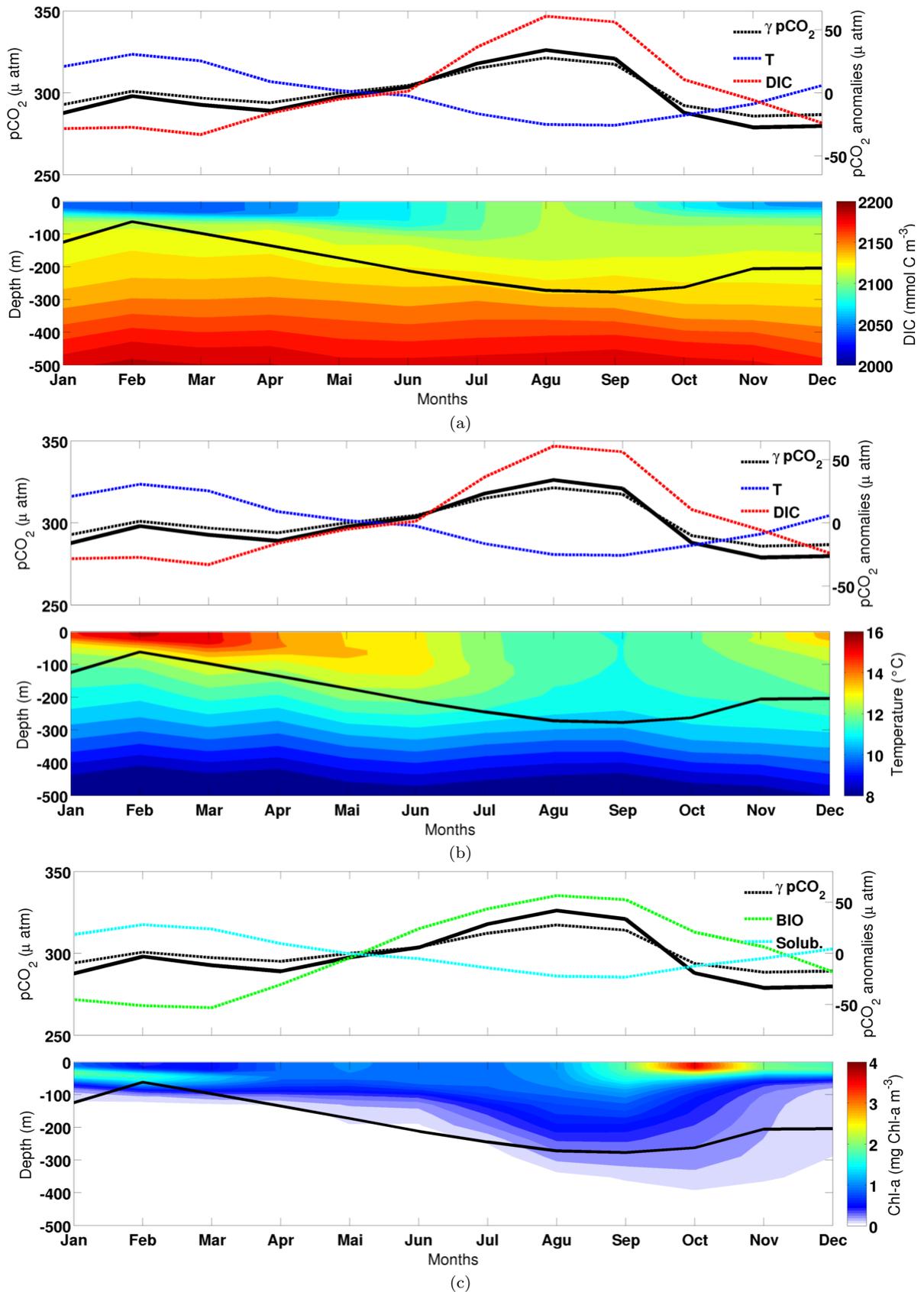
**Figure 13.** Vertical profile at 42°S, 42°W. Upper panels showing monthly mean surface $p$CO$_2$ (solid black line), $p$CO$_2$ anomalies (dashed black line) and the contribution from $T$ and $DIC^s$ (red and blue dashed lines) and the contribution of biology and solubility (green and cyan dashed lines). Lower panels showing vertical profiles of $DIC$ (a), $T$ (b), and chlorophyll a(c), black line represents the mixed layer depth.
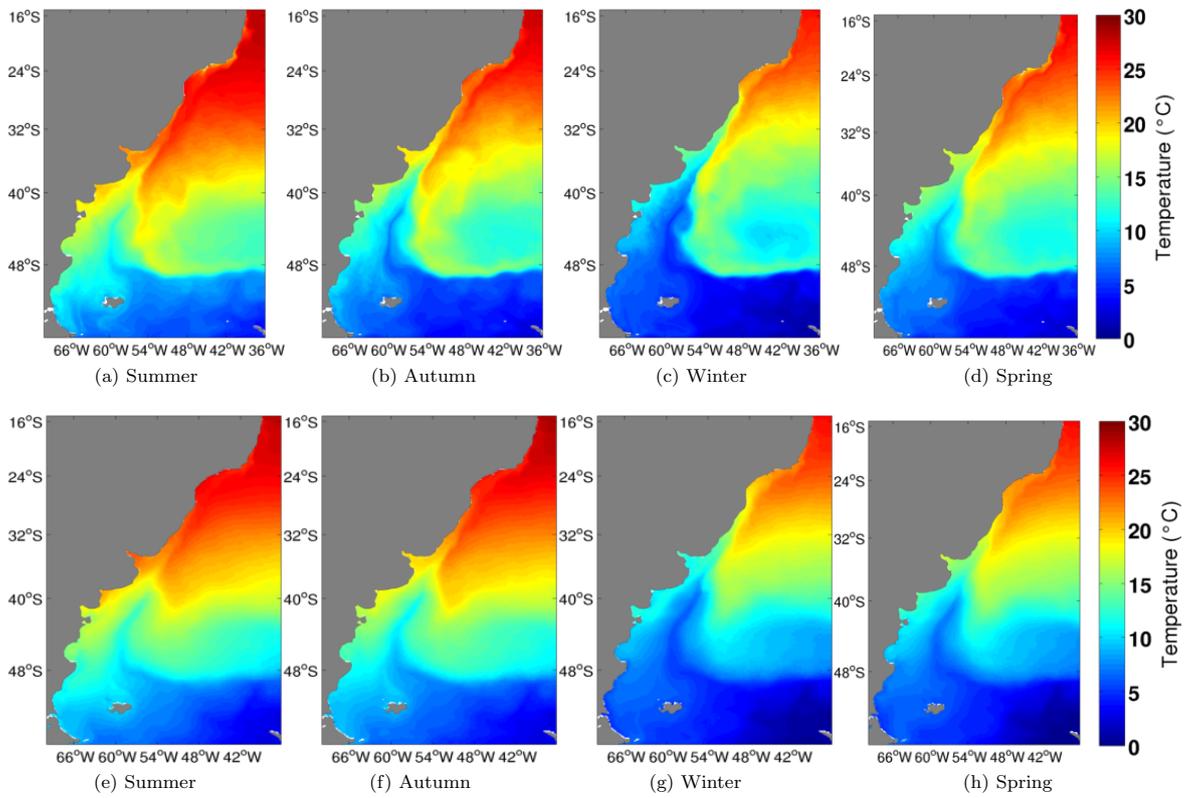
**Figure 14.** Seasonal climatology of modeled sea surface temperature °C - 4 years average (upper row), and climatology from AVHRR sensor - from 1985 to 2002 (lower row).
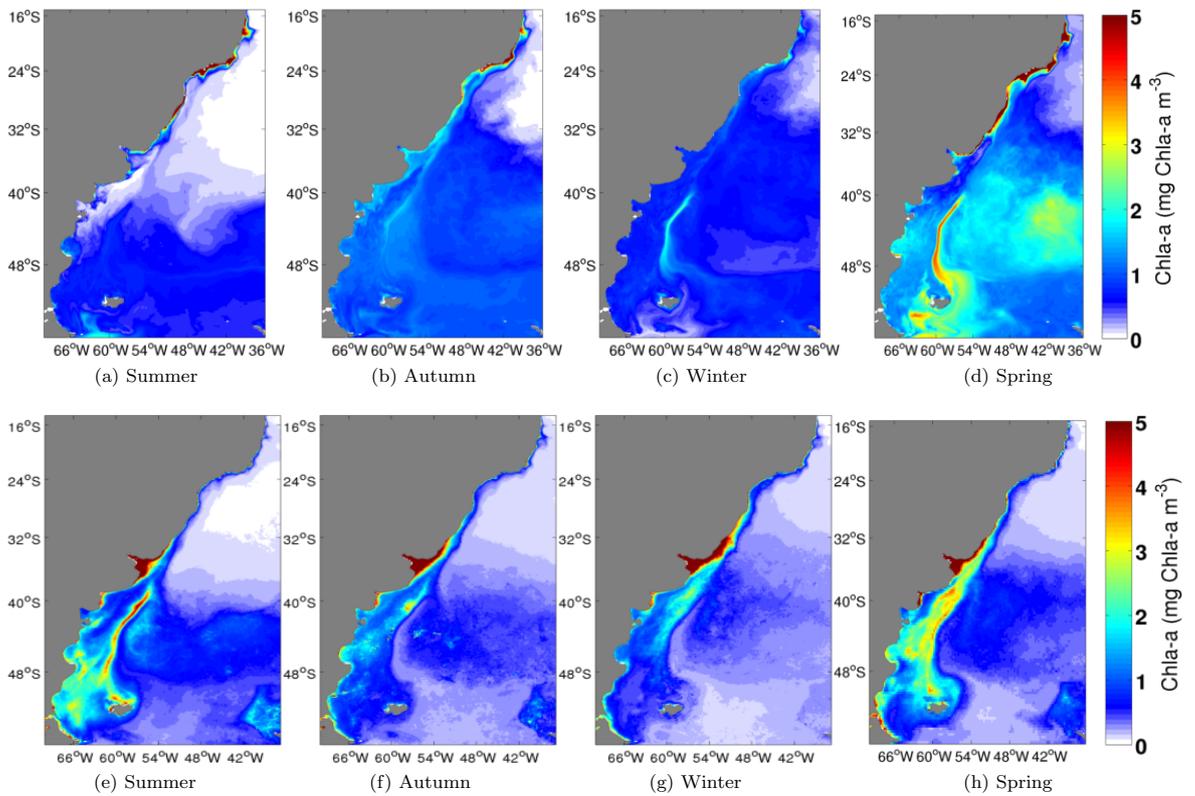
**Figure 15.** Seasonal climatology of modeled chlorophyll-a concentration mgChla-a m$^{-3}$ - 4 years average (upper row), and climatology from Aqua-Modis sensor - from 2003 to 2013 (lower row).